Error Vector Magnitude Analysis for OFDM Systems

Chunming Zhao and Robert J. Baxley
School of Electrical and Computer Engineering, Georgia Tech, Atlanta, GA 30332-0250, USA

***Abstract*— Error vector magnitude (EVM) is a popular figure-of-merit adopted by various communication standards for evaluating in-band distortions introduced in a communication system. In this paper, we regard EVM as a random variable and investigate its statistical distributions as the result of the following distortion mechanisms: phase noise, amplitude clipping, power amplifier nonlinearities, and gain/phase imbalances in orthogonal frequency division multiplexing (OFDM) systems. We relate key parameters characterizing the various distortion mechanisms to the statistical behavior of EVM; such statistical behavior can be used to verify compliance of the transmit signals to the requirements of the standard.**

I. Introduction

Error vector magnitude (EVM) is a popular figure-of-merit for evaluating in-band distortions introduced in a communication system. Compared with bit error rate (BER), EVM not only quantifies the distortions, but also attributes the source of distortion to phase noise, modulator imbalances, power amplifier nonlinearities, and so on [1], [2]. EVM is more useful than bit error rate (BER) when performing the real-world RF design and troubleshooting. A number of studies on simulations and measurements of EVM have been proposed [3], [4], [5]. EVM analysis for distortions in an 8-PSK system, a GSM EDGE system, a wideband code division multiple access (CDMA) system, and a general linear single-carrier transmit-receive system have been investigated in [6], [7] [8], and [9], respectively. With its excellent troubleshooting capability, EVM has been adopted by many communication standards, such as wideband CDMA, wireless LAN, and wireless MAN [10]. EVM has also been taken into account when formulating peak-to-average power ratio (PAR) reduction algorithms, such as in [11], [12].

The objectives of the present study are twofold. First, we will carry out statistical analyses of the EVM for various distortion mechanisms. Second, we will apply our derived theoretical results to check whether the EVM of OFDM signals satisfies the standard requirement. It is anticipated that our proposed theoretical derivations will simplify OFDM EVM evaluation by avoiding the necessity of costly hardware tests and/or software simulations.

The outline of this paper is as follows. Section II presents the definition of EVM and derives its approximated distribution in the Wireless MAN OFDM scenario [10]. From Section III to Section VI, we calculate statistical parameters of EVM for the following distortion mechanisms: phase noise, amplitude clipping, power amplifier (PA) nonlinearities, and gain/phase imbalances. Based on the derived statistical behaviors of EVM, RF designers can easily calculate how much specific distortions can be endured in a system. Conclusions are drawn in Section VII.

II. EVM and its Approximated Distribution

Fig. 1 illustrates the EVM concept. Denote by X_k the reference signal, Y_k its distorted version, and $D_k = Y_k - X_k$ the error signal (vector). The so-called EVM is defined as [10]:

$$EVM = \sqrt{\frac{\frac{1}{N}\sum_{k=0}^{N-1}|Y_k - X_k|^2}{S_{\max}^2}} = \sqrt{\frac{\frac{1}{N}\sum_{k=0}^{N-1}|D_k|^2}{S_{\max}^2}}, \tag{1}$$

where $S_{\max}$ is the maximum amplitude of the constellation points that define X_k, and N is the number of points in a measurement. Since X_k is a random variable, EVM is a random variable as well. In this paper, we will focus on

$$Z = \frac{1}{N}\sum_{k=0}^{N-1}\frac{|D_k|^2}{S_{\max}^2}, \tag{2}$$

which conveys information about sample-averaged normalized error powers.

Two related parameters are the magnitude error $E_k = |Y_k| - |X_k|$ and the phase error $\phi_k = \angle Y_k - \angle X_k$, which are useful to identify the phase-related distortion.

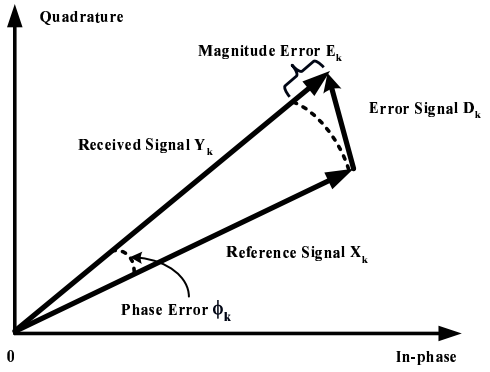

Fig. 1. Illustration of the EVM definition.

We will focus on orthogonal frequency division multiplexing (OFDM) systems. The time-domain OFDM signal $x_n, 0 \le n \le N-1$, is generated from X_k, the modulated symbol on the kth subcarrier, through the inverse discrete

Fourier transform (IDFT),

$$x_n = IDFT\{X_k\} = \frac{1}{\sqrt{N}} \sum_{k=0}^{N-1} X_k \; e^{j2\pi nk/N}, \qquad (3)$$

where N is the number of subcarriers in one OFDM symbol. When N is large, the real and imaginary parts of x_n are approximately i.i.d. Gaussian distributed with zero mean and variance σ^2. Also, we have $\mathcal{E}[|X_k|^2] = \mathcal{E}[|x_n|^2] = 2\sigma^2$ where $\mathcal{E}[\cdot]$ is the expectation operation.

Denote by $d_n = y_n - x_n$ ($d_n = IDFT\{D_k\}$ and $y_n = IDFT\{Y_k\}$) the error vector in the time domain. Using the Parseval's Theorem, we can rewrite (2) as

$$Z = \frac{1}{N} \sum_{n=0}^{N-1} \frac{|d_n|^2}{S_{\max}^2}. \qquad (4)$$

During transmission, the OFDM signal x_n may experience various distortions. The standards specify limits on the EVM to ensure satisfactory in-band performance. For example, the IEEE 802.16 standard [10], for which OFDM is one of the candidates for physical layer transmission, specifies that the EVM threshold is 12% if X_k is QPSK, or 6% if X_k is 16QAM [10]. If the dB scale is concerned, $\mathcal{E}[Z]$ should not exceed -18.4dB for QPSK, or -24.4dB for 16QAM.

Observing (2) and (4), we can find that Z is composed of the summation of N random variables with identical distribution. Suppose these random variables are also independent, then the central limit theorem can be applied when N is large. Thus, Z approximates the Gaussian distribution with the probability density function

$$f_Z(z) = \frac{1}{\sqrt{2\pi}\zeta} e^{-\frac{(z-\mu)^2}{2\zeta^2}}, \qquad (5)$$

where $\mu = \mathcal{E}[Z] = \mathcal{E}[|d_n|^2]/S_{max}^2$ is the mean and $\zeta^2 = Var[Z] = Var[|d_n|^2]/(N \cdot S_{max}^4)$ is the variance ($Var[\cdot]$ is the variance operation). For various distortion mechanisms, we only need to calculate μ and ζ^2 to obtain the distribution of Z. Similar results were given in [13] that presented the distribution through simulations for wireless LAN systems.

A series troubleshooting measurements were presented in [1], [2] to identify the distortion source according to different symptoms. Detailed μ values are calculated for different distortions in the following sections. We will then demonstrate that it is possible to use the EVM-related parameters to diagnose the source of distortion. Also, based on theoretical values of μ, we are able to derive the limiting values for phase noise, PA clipping level, PA non-linearity coefficient and gain/phase imbalance that result in permissable EVM.

III. EVM Analysis of Phase Noise

It is said in [1]: "Different error mechanisms will affect a signal in different ways, perhaps in magnitude only, phase only, or both simultaneously.... Thus, the first diagnostic step is to resolve EVM into its magnitude and phase error components and compare their relative sizes." So when $\mathcal{E}[|\phi_k|] >> \mathcal{E}[|E_k|]$, some sort of unwanted phase distortion is the dominant error. However, the inverse statement is not always true for OFDM systems [2], i.e., phase noise may not always have $\mathcal{E}[|\phi_k|] >> \mathcal{E}[|E_k|]$. We will demonstrate this using the phase noise distortion mechanism.

From [14], the baseband phase noise model is

$$y_n = x_n \cdot e^{j\theta_n}, \qquad (6)$$

where θ_n is the phase noise at the nth sample. Suppose θ_n is small, so that $e^{j\theta_n} \approx 1 + j\theta_n$. Then, in the frequency domain, we have $Y_k = X_k + jX_k\Theta + ICI_k$, where $\Theta = 1/\sqrt{N}\sum_{n=0}^{N-1}\theta_n$ is the common phase error (CPE), and ICI_k is the intercarrier interference (ICI) at the kth subcarrier.

When the phase noise variations are much slower than the OFDM period, the CPE dominates over the ICI. In this case, $Y_k = X_k(1 + j\Theta)$, hence we have $|E_k| = ||Y_k| - |X_k|| = |X_k|(\sqrt{1+\Theta^2} - 1)$ and $|\phi_k| = |\angle Y_k - \angle X_k| = \tan^{-1}\Theta$. When Θ is small, $\mathcal{E}[|E_k|] \approx 0 << \mathcal{E}[|\phi_k|] \approx \Theta$. So the condition $\mathcal{E}[|\phi_k|] >> \mathcal{E}[|E_k|]$ is satisfied no matter what the modulation scheme is used.

If both the CPE and the ICI should be considered, the analysis becomes complicated, hence we rely on the simulation to check the relationship between $\mathcal{E}[|\phi_k|]$ and $\mathcal{E}[|E_k|]$. From [14], θ_n can be regarded as Gaussian distributed with zero mean and variance σ_θ^2. Define $\lambda = \mathcal{E}[|\phi_k|]/\mathcal{E}[|X_k|]$, which is larger than 5 when we say $\mathcal{E}[|\phi_k|] >> \mathcal{E}[|E_k|]$ [1]. Shown in Fig. 2 are the λ curves changing with σ_θ^2 for various modulation schemes. Clearly, we can only say that $\mathcal{E}[|\phi_k|] >> \mathcal{E}[|E_k|]$ for the BPSK modulation. For QPSK and 16QAM modulation schemes, the average phase error and the average magnitude error are in similar levels.

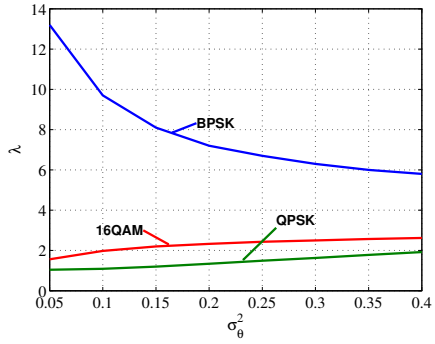

Fig. 2. Relationship between $\lambda = \mathcal{E}[|\phi_k|]/\mathcal{E}[|X_k|]$ and the phase noise variance, $N = 2048$.

Suppose $|E_k| \approx 0$, i.e. $|Y_k| \approx |X_k|$, we can calculate the EVM as the result of the phase distortion as

$$Z = \frac{1}{N} \sum_{k=0}^{N-1} \frac{2(1 - \cos\phi_k)|X_k|^2}{S_{\max}^2}. \qquad (7)$$

Because ϕ_k and $|X_k|$ are independent random variables, we

can calculate

$$\mu = \frac{2(1-\mathcal{E}[\cos\phi_k])\mathcal{E}[|X_k|^2]}{S_{\max}^2} = \frac{2(1-\mathcal{E}[\cos\phi_k])}{\gamma}, \quad (8)$$

where $\gamma = S_{\max}^2/(2\sigma^2)$ is the PAR of the constellation for X_k. Phase noise ϕ_k is assumed to be a Gaussian random variable with zero mean and variance σ_ϕ^2, so [15, page 483]

$$\mathcal{E}_{\phi_k}[\cos\phi_k] = \int_{-\infty}^{+\infty} \cos\phi_k \cdot \frac{1}{\sqrt{2\pi}\sigma_\phi} e^{-\frac{\phi_k^2}{2\sigma_\phi^2}} d\phi_k = e^{-\frac{\sigma_\phi^2}{2}}. \quad (9)$$

Hence,

$$\mu = \frac{2(1-e^{-\frac{\sigma_\phi^2}{2}})}{\gamma}. \quad (10)$$

By observing (10), we find that μ increases with the phase noise power σ_ϕ^2. In Fig. 3, μ vs. σ_ϕ^2 for different modulation schemes are shown. To satisfy the requirement of the standard, σ_ϕ^2 should be less than or equal to 0.014, 6.5×10^3 and 2.1×10^3 for QPSK, 16QAM and 64QAM respectively.

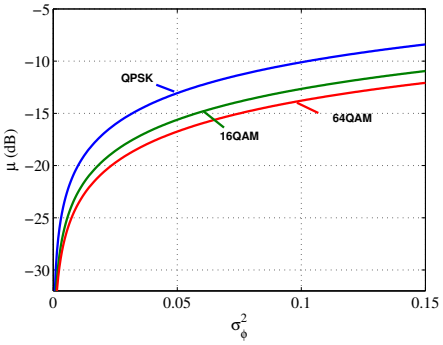

Fig. 3. Theoretical μ with different σ_ϕ^2 values.

IV. EVM Analysis of Amplitude Clipping

OFDM is an attractive multi-carrier transmission scheme which is capable of resisting multi-path fading and inter-symbol interference. However, due to the Gaussianity of x_n as shown in (3), PAR of x_n is usually large, which will drive the power amplifier (PA) in to its nonlinear region incurring undesirable in-band and out-of-band distortions. Scaling the high PAR signal can reduce distortions at the cost of lower PA efficiency. Hence, PAR reduction algorithms are called for to improve the power efficiency of the PA while keeping the distortions low.

Distortion PAR reduction methods, such as time-domain clipping, deliberately introduce distortions at the baseband to reduce the dynamic range of the input signal. EVM is an excellent in-band distortion metric and should be evaluated in the PAR reduction process [11], [12].

On the other hand, the peak amplitude limitation of PA can also be modeled as an amplitude clipping operation. So clipping is an important and frequently encountered distortion source. The clipped time-domain signal can be written as

$$y_n = \begin{cases} x_n, & |x_n| \le A \\ Ae^{j\angle x_n}, & |x_n| > A \end{cases}, \quad (11)$$

where A is the clipping threshold.

The magnitude of the time-domain clipping noise d_n is

$$|d_n| = |y_n - x_n| = \begin{cases} 0, & r \le A \\ |x_n| - A, & |x_n| > A \end{cases}, \quad (12)$$

where $|x_n|$ has the Rayleigh distribution $f_{|x_n|}(r) = \frac{r}{\sigma^2}e^{-r^2/2\sigma^2}, r \ge 0$.

Hence, the average power of the clipping noise d_n is

$$\begin{aligned}\mathcal{E}[|d_n|^2] &= \int_A^\infty (r-A)^2 f_{|x_n|}(r)dr \\ &= 2\sigma^2 e^{-A^2/2\sigma^2} - \sigma A\sqrt{2\pi}\ \mathrm{erfc}\left(\frac{A}{\sigma\sqrt{2}}\right). \end{aligned} \quad (13)$$

Substituting (13) into (4), we obtain

$$\mu = \frac{\mathcal{E}[|d_n|^2]}{S_{max}^2} = \frac{e^{-A^2/2\sigma^2}}{\gamma} - \frac{\frac{A}{\sigma}\sqrt{\frac{\pi}{2}}\ \mathrm{erfc}(\frac{A}{\sigma\sqrt{2}})}{\gamma}. \quad (14)$$

The result in (13) was also derived in [8] using a conditional probability method.

Fig. 4 presents theoretical values of μ when the number of subcarriers N is 128. The solid line is obtained from (14) for the QPSK constellation ($\sigma = 1$, $S_{\max} = \sqrt{2}$), while the dashed line is for the 16QAM constellation ($\sigma = \sqrt{5}$, $S_{\max} = \sqrt{18}$). If we are to use (14) to select the clipping ratio $\Omega = \frac{A}{2\sigma}$ to meet 802.16 EVM requirements [10], we find that $\Omega \ge 3.6$dB for QPSK and $\Omega \ge 4.6$dB for 16QAM are necessary.

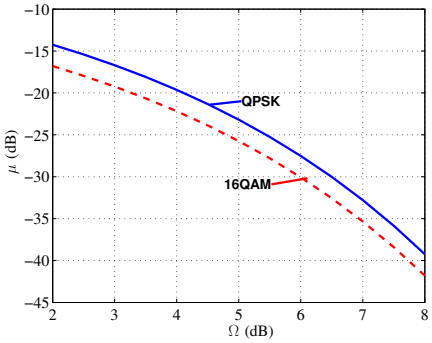

Fig. 4. Theoretical μ as a function of the clipping ratio.

V. EVM analysis of Base-Band Polynomial Model for Nonlinearities of the PA

Power amplifier (PA) is an essential component in communications systems. However, the nonlinearity that is inherent in PAs introduces in-band distortion and out-of-band spectral regrowth. Baseband polynomial model is a convenient way to describe nonlinearities [16].

The baseband polynomial model including both the odd-order and the even-order terms can be written as [17]

$$y_n = \sum_{k=1}^{K} b_k \; x_n \; |x_n|^{k-1}, \tag{15}$$

where x_n is the baseband PA input signal, y_n is the baseband PA output signal, K is the polynomial order which is an integer, and b_k are polynomial coefficients.

The time-domain nonlinear distortion can be written as

$$d_n = \sum_{k=1}^{K} \frac{b_k}{b_1} \; x_n \; |x_n|^{k-1} - x_n = \sum_{k=2}^{K} c_k \; x_n \; |x_n|^{k-1}, \tag{16}$$

where $c_k = b_k/b_1, \forall k \geq 2$.

The magnitude square of d_n can be further expressed as

$$\begin{aligned} |d_n|^2 &= \left| \sum_{k=2}^{K} c_k \; x_n \; |x_n|^{k-1} \right|^2 \\ &= \left(\sum_{k=2}^{K} c_k \; |x_n|^{k-1} \right) \cdot \left(\sum_{l=2}^{K} c_l \; |x_n|^{l-1} \right)^* \cdot |x_n|^2 \\ &= \sum_{k=2}^{K} \sum_{l=2}^{K} c_k \; c_l^* \; |x_n|^{k+l}, \end{aligned} \tag{17}$$

where $(\cdot)^*$ is the complex conjugate operation.

Because $|x_n|$ has the Rayleigh distribution, the mth order moment of $|x_n|$ is [18, page 148]

$$\mathcal{E}[|x_n|^m] = 2^{\frac{m}{2}} \Gamma\left(\frac{m+2}{2}\right) \sigma^m = \begin{cases} m!!\sigma^m, & m \text{ even}, \\ \sqrt{\frac{\pi}{2}} m!!\sigma^m, & m \text{ odd}, \end{cases} \tag{18}$$

where $\Gamma(\cdot)$ is the Gamma function and $(.)!!$ is the double factorial operation. By combining (17) and (18), we can calculate the statistical expectation of Z as

$$\begin{aligned} \mu &= \frac{\mathcal{E}[|d_n|^2]}{S_{max}^2} = \frac{\sum_{k=2}^{K} \sum_{l=2}^{K} c_k \; c_l^* \; \mathcal{E}[|x_n|^{k+l}]}{S_{max}^2} \\ &= \frac{\sum_{k=2}^{K} \sum_{l=2}^{K} c_k \; c_l^* \; 2^{\frac{k+l}{2}} \Gamma(\frac{k+l+2}{2}) \sigma^{k+l}}{S_{max}^2}. \end{aligned} \tag{19}$$

If the band-pass signal is of interest, we only need to consider the odd-order polynomial terms in (15). In this case, the polynomial coefficients $b_k, k = 1, 3, \cdots, K$ are real numbers for strictly memoryless PA and complex numbers for quasi-memoryless PA. Hence, (19) becomes

$$\mu = \frac{\sum_{k=3,\; k \text{ odd}}^{K} \sum_{l=3,\; l \text{ odd}}^{K} c_k c_l^* (k+l)!! \sigma^{k+l-2}}{\gamma}. \tag{20}$$

From (20), we can observe that the distortion depends on the signal variance, the polynomial coefficients and the polynomial order. For example, if only the third order nonlinearity is present, we have $\mu = 24|c_3|^2\sigma^4/\gamma$. Hence, EVM would increase with the degree of nonlinearity $|c_3|^2$. The polynomial coefficients can be obtained from either measured AM/AM and AM/PM curves of the PA by applying the polynomial fitting, or the odd-order intercept points and 1-dB compression point by solving a system of equations [16].

To demonstrate the relationship between μ and related parameters, we present numerical examples by setting σ^2 to be one. For a fixed $c_3 = -0.02$, μ decreases with γ. Three γ's corresponding to QPSK, 16QAM and 64QAM are shown in Fig. 5. By comparing μ with the threshold, we find that only the QPSK satisfies the requirement of the standard when $c_3 = -0.02$. For the 16QAM and 64QAM constellations, $|c_3|$ must be smaller than 0.02 to meet the EVM requirement.

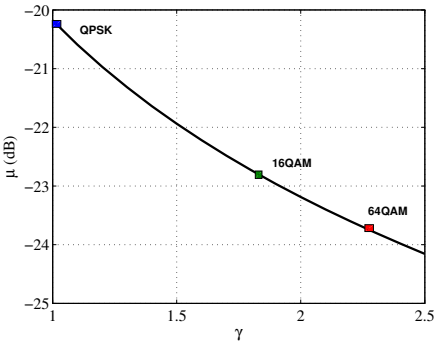

Fig. 5. Theoretical μ with different γ values, where $c_3 = -0.02$.

Shown in Fig. 6 is the relationship between μ and $|c_3|$ for different modulation schemes. To satisfy the requirement of the standard, $|c_3|$ should not be larger than 0.025, 0.017 and 0.009 for QPSK, 16QAM and 64QAM respectively.

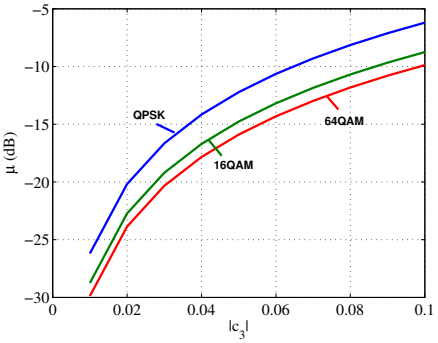

Fig. 6. Theoretical μ with different $|c_3|$ values.

VI. EVM Analysis of Gain/Phase Imbalances

Gain/phase imbalances occur in the front-end analog processing that will distort the in-band OFDM signal [19], [20]. The imbalances can be characterized by two parameters: the gain imbalance ϵ and the phase imbalance $\Delta\phi$. The baseband model can be written as:

$$y_n = \alpha \cdot x_n + \beta \cdot x_n^*, \tag{21}$$

where $\alpha = \cos\Delta\phi + j\epsilon \sin\Delta\phi$ and $\beta = \epsilon\cos\Delta\phi - j\sin\Delta\phi$. If no imbalance exists, i.e., $\epsilon = 0$, $\Delta\phi = 0$, then $\alpha = 1$ and $\beta = 0$ and (21) reduces to $y_n = x_n$.

The distortion signal can be expressed as $d_n = y_n - x_n = \eta \cdot x_n + \beta \cdot x_n^*$, where $\eta = \alpha - 1$. So the distortion power is

$$\begin{aligned} \mathcal{E}[|d_n|^2] &= \mathcal{E}\left[(\eta \cdot x_n + \beta \cdot x_n^*) \cdot (\eta \cdot x_n + \beta \cdot x_n^*)^*\right] \\ &= (|\eta|^2 + |\beta|^2)\mathcal{E}[|x_n|^2] + \eta\beta^*\mathcal{E}[x_n^2] + \eta^*\beta\mathcal{E}[(x_n^*)^2]. \quad (22) \end{aligned}$$

Based on the assumption that x_n is circular complex Gaussian distributed, $\mathcal{E}[x_n^2] = \mathcal{E}[(x_n^*)^2] = 0$. Hence,

$$\mu = \frac{|\eta|^2 + |\beta|^2}{\gamma} = \frac{\epsilon^2 + 2(1 - \cos\Delta\phi)}{\gamma}. \quad (23)$$

The contours of μ with different gain and phase imbalances are plotted in Fig. 7 for the QPSK modulation. We can see that EVM increases with gain/phase imbalances. The regions below the solid line indicate the allowed gain/phase imbalances combinations to satisfy the standard's requirements.

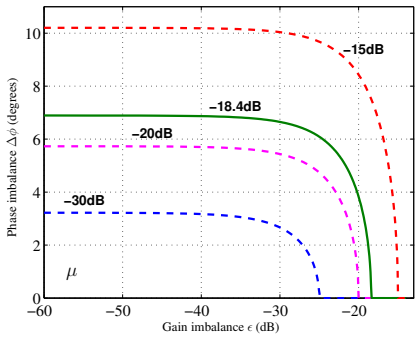

Fig. 7. Theoretical μ contours with different gain and phase imbalances for the QPSK modulation.

The symptom of gain/phase imbalances in OFDM systems is the constellation state spreading, which is different from that of the single-carrier systems [2]. Hence, it is difficult to differentiate the gain/phase imbalances from other distortions for high-order modulation schemes. Rather, it is preferred to observe the constellation diagram of the pilot subcarriers, which are BPSK modulated, in order to diagnose the problem.

When only the phase imbalance exists, i.e., $\alpha = \cos\Delta\phi$ and $\beta = -j\sin\Delta\phi$, we have $Y_k = \alpha X_k + \beta X_k^{\#}$, where $X_k^{\#} = X_{(N-k) \bmod N}^*$ and $(\cdot)^*$ is the complex conjugate operation. For the BPSK symbols, $X_k^{\#} = X_{(N-k) \bmod N}$ and $|X_k^{\#}| = |X_k|$. Hence, $|Y_k| \equiv |X_k|$ that implies $E_k \equiv 0$. On the other hand, $|\phi_k| \equiv \Delta\phi$. So the condition $\mathcal{E}[|\phi_k|] >> \mathcal{E}[|E_k|]$ is satisfied. Hence, we can judge the distortion source to the phase imbalance by comparing $|\phi_k|$ and $|E_k|$ of the BPSK pilot signals.

VII. Conclusions

In this paper, we analyzed statistical behaviors of EVM caused by various impairments including phase noise, amplitude clipping, PA nonlinearities and gain/phase imbalances. Theoretical μ values for some specific distortion mechanisms were calculated for the various impairments. The results were twofold: first, based on the relationship between the phase error and the magnitude error, we demonstrated how the source of the distortion could be diagnosed; second, using the theoretical calculations, we provided concrete thresholds for the amount of allowable distortions from each distortion source in order to meet EVM requirements.

References

[1] "Using error vector magnitude measurements to analyze and troubleshoot vector-modulated signals," Agilent PN 89400-14 Product Note, Agilent Technologies.

[2] B. Cutler, "Effects of physical layer impairments on OFDM systems," *RF Design*, pp. 36–44, May 2002.

[3] H. Ku, *Behavioral modeling of nonlinear RF power amplifiers for digital wireless communication systems with implications for predistortion linearization systems*. PhD thesis, Oct. 2003.

[4] S. Yamanouchi, K. Kunihiro, and H. Hida, "An efficient algorithm for simulating error vector magnitude in nonlinear OFDM amplifiers," *Proc. IEEE Custom Integrated Circuits Conference*, pp. 129–132, Oct. 2004.

[5] J. H. Kim, J. H. Jeong, S. M. Kim, C. S. Park, and K. C. Lee, "Prediction of error vector magnitude using AM/AM, AM/PM distortion of RF power amplifier for high order modulation OFDM system," *Proc. IEEE MTT-S International Microwave Symposium Digest*, pp. 2027–2030, June 2005.

[6] J. L. Pinto and I. Darwazeh, "Error vector magnitude relation to magnitude and phase distortion in 8-PSK systems," *IEE Electronics Letters*, vol. 37, pp. 437–438, Mar. 2001.

[7] A. Mashhour and A. Borjak, "Method for computing error vector magnitude in GSM EDGE systems – simulation results," *IEEE Communications Letters*, vol. 5, no. 3, pp. 88–91, Mar. 2001.

[8] O. Vaananen, J. Vankka, and K. Halonen, "Effect of baseband clipping in wideband CDMA system," *Proc. IEEE Seventh International Symposium on Spread Spectrum Techniques and Applications*, vol. 2, pp. 445–449, Sept. 2002.

[9] A. Georgiadis, "Gain, phase imbalance, and phase noise effects on error vector magnitude," *IEEE Trans. on Vehicular Technology*, vol. 53, no. 2, pp. 443–449, Mar. 2004.

[10] "IEEE standard for local and metropolitan area networks part 16: Air interface for fixed broadband wireless access systems," *IEEE Std 802.16-2004 (Revision of IEEE Std 802.16-2001)*, pp. 1–857, 2004.

[11] A. Aggarwal and T. H. Meng, "Minimizing the peak-to-average power ratio of OFDM signals using convex optimization," *IEEE Trans. on Signal Processing*, vol. 54, no. 8, pp. 3099–3110, Aug. 2006.

[12] R. J. Baxley, C. Zhao, and G. T. Zhou, "Constrained clipping for crest factor reduction in OFDM," *IEEE Trans. on Broadcasting, accepted*.

[13] K. Rai, "On using error vector magnitude as a figure of merit for multicarrier communication systems," *EE359 Course Project, Stanford University*, Dec. 2005.

[14] S. Wu and Y. Bar-Ness, "OFDM systems in the presence of phase noise: consequences and solutions," *IEEE Trans. on Communications*, vol. 52, no. 11, pp. 1988–1996, Nov. 2004.

[15] I. S. Gradshteyn, I. M. Ryzhik, A. Jeffrey, and D. Zwillinger, *Table of Integrals, Series, and Products*. Academic Press, 6 ed., July 2000.

[16] G. T. Zhou and J. S. Kenney, "Predicting spectral regrowth of nonlinear power amplifiers," *IEEE Trans. on Communications*, vol. 50, no. 5, pp. 718–722, May 2002.

[17] L. Ding and G. T. Zhou, "Effects of even-order nonlinear terms on power amplifier modeling and predistortion linearization," *IEEE Trans. on Vehicular Technology*, vol. 53, no. 1, pp. 156–162, Jan. 2004.

[18] A. Papoulis and S. U. Pillai, *Probability, Random Variables and Stochastic Processes*. McGraw-Hil, 4 ed., Dec. 2001.

[19] J. Tubbax, B. Come, L. V. Perre, S. Donnay, M. Engels, H. D. Man, and M. Moonen, "Compensation of IQ imbalance and phase noise in OFDM systems," *IEEE Trans. on Wireless Communications*, vol. 4, no. 3, pp. 872–877, May 2005.

[20] A. Tarighat, R. Bagheri, and A. H. Sayed, "Compensation schemes and performance analysis of IQ imbalance in OFDM receivers," *IEEE Trans. on Signal Processing*, vol. 53, no. 7, pp. 3257–3268, July 2005.